chemosensors

MDPI

Communication

Measuring Water Vapor Sorption Hysteresis of Cement Paste through an Optical Fiber Sensor

Pedro M. da Silva [1,2], Luís C. C. Coelho [1,*] and José M. M. M. de Almeida [1,3]

[1] INESC TEC—Institute of Systems and Computer Engineering, Technology and Science, Faculty of Sciences, University of Porto, Rua do Campo Alegre, 4169-007 Porto, Portugal
[2] Faculty of Engineering, University of Porto, Rua Doutor Roberto Frias, 4200-465 Porto, Portugal
[3] Department of Physics, School of Sciences and Technology, University of Trás-os-Montes e Alto Douro, 5001-801 Vila Real, Portugal
* Correspondence: luis.c.coelho@inesctec.pt

Abstract: Water vapor sorption is a powerful tool for the analysis of cement paste, one of the most used substances by mankind. The monitoring of cementitious materials is fundamental for the improvement of infrastructure resilience, which has a deep impact on the economy, the environment, and on society. In this work, a multimode fiber was embedded in cement paste for real-time monitoring of cement paste water vapor sorption. Changes in the reflected light intensity due to the build-up of water in the cement paste's pores were exploited for this purpose. The sample was 7-day moist cured, and the relative humidity was controlled between 8.9% and 97.6%. Reflected light intensity was converted into a specific surface area of cement paste (133 m^2/g) and thickness of water through the Brunauer-Emmett-Teller (BET) method and into a pore size distribution through the Barret-Joyner-Halenda (BJH) method. The results achieved through reflected light intensity agree with those found in the literature, validating the usage of this setup for the monitoring of water vapor sorption, breaking away from standard gravimetric measurements.

Keywords: fiber optic sensors; cement paste; characterization; water vapor sorption; real-time monitoring; hysteresis; sorption isotherm

check for updates

Citation: da Silva, P.M.; Coelho, L.C.C.; de Almeida, J.M.M.M. Measuring Water Vapor Sorption Hysteresis of Cement Paste through an Optical Fiber Sensor. *Chemosensors* **2023**, *11*, 123. https://doi.org/10.3390/chemosensors11020123

Academic Editor: Mateusz Smietana

Received: 3 January 2023
Revised: 29 January 2023
Accepted: 2 February 2023
Published: 7 February 2023

Copyright: © 2023 by the authors. Licensee MDPI, Basel, Switzerland. This article is an open access article distributed under the terms and conditions of the Creative Commons Attribution (CC BY) license (https://creativecommons.org/licenses/by/4.0/).

1. Introduction

Concrete is the second most used material by mankind [1]. It permeates most of humanity's infrastructures, and it is a cornerstone for human development [2]. Its main constituent is cement, whose binding properties when mixed with water, confer to concrete its compressive strength. Knowledge of the behavior of cementitious materials and the mechanics of their decay is critical to our society, especially when considering the nefarious social, economic, and environmental [1] impacts that the premature decay of these infrastructures could have. The demand for devices capable of real-time structural health monitoring of reinforced concrete structures is ever-growing [3].

Water is vital to cement paste throughout its life cycle. The quantity and availability of water in the beginning and during cement paste mixing and curing will define its long-lasting properties [4,5]. Water is also a requirement for several decaying mechanisms of cement paste, thus, being a major influencer on cement paste's expiry. For this reason, the rate of water uptake is a measure of cement paste durability [6], but it can also be used as a molecular probe of cement paste through water vapor sorption [6,7].

Sorption isotherms are a technique of cement paste characterization wherein, under an atmosphere with a given stable relative humidity (RH), the amount of water in the pores of cement paste will change until an equilibrium is reached. This equilibrium can be measured through the gravimetric measurements of the sample, and from these measurements, a slew of properties can be accessed and used in the modeling of cement paste decay, such as porosity, specific surface area, number of calcium-silicate-hydrates, pore size distribution

and connectivity, and water transport properties [7]. Cement paste, due to its mesopores (2–50 nm), exhibits hysteresis in its water vapor sorption [7,8]. Saturated salt solutions are used to produce an atmosphere with stable RH [9], with the sample being weighed once its mass has stabilized [10]. A 3 mm thick cement paste sample could require several months to reach equilibrium under a given RH. This technique can also employ nitrogen as an absorbate instead of water, albeit the minimum pore size reached is slightly decreased [11]: water sorption operates between 0.5 nm and 25 µm, while nitrogen sorption reaches 1 nm to 50 µm.

Gravimetric measurements of water sorption can be achieved in 24 h through dynamic vapor sorption [12]. In this method, the RH is controlled with two gas inlets: one for dry air and one for moist air. The agitation of the gas caused by the two gas inlets is responsible for the time saved in data acquisition. If the sample has not reached an equilibrium with the outside RH within 24 h, an estimation of the total absorption is made.

Volumetric measurements can be used for sorption isotherms as an alternative to gravimetric measurements. This is performed by measuring the change in pressure of a known amount of gas that is partially absorbed into the sample [13]. Unlike gravimetric measurements, pretreatment of the sample is required in the volumetric method. The sample is crushed into a powder, so a vacuum is achieved at the start of the method.

Sorption isotherms reach a minimum pore size of 0.5 nm, which is lower than the 4 nm reached by mercury intrusion porosimetry (MIP) and the 100 nm of a scanning electron microscope (SEM). It comes close to the 0.2 nm of proton nuclear magnetic resonance relaxometry (H-NMR) [11]. This resolution makes sorption isotherms ideal for the study of cement paste, whose calcium silica layers are spaced between 0.1–1 nm, and gel pores are sized between 2–10 nm [14].

Cement paste and other cementitious materials have been extensively researched throughout the past decade [2], and yet, characterization methods of cement paste remain an important area of research. These methods present more than a means for analysis of current infrastructure; they are key in characterizing new cementitious materials [15,16] that aim to improve the performance, durability, and environmental impact of concrete. Furthermore, the characterization of cement paste is heavily influenced by the characterization method used, with several works being devoted to explaining these differences [13,17–19]. Different characterization methods of cement paste use different interaction phenomena between the probing method and the cement paste. New methods of characterization comprise new opportunities for reaching new knowledge about cementitious materials.

In the present work, a new method of sorption isotherms based on light reflectance is proposed for cement paste characterization. A polished multimode fiber tip was embedded in cement paste and was successfully used to monitor changes in reflection intensity caused by the adsorption and desorption of water in cement paste at different RHs. Through this monitoring, the specific surface area and pore size distribution of cement paste were achieved.

2. Materials and Methods

A polished silica core multimode fiber tip (MMF-117FT600UMT, Thorlabs, Dortmund, Germany), with 600 µm core diameter, was dipped in and removed from a recently and thoroughly mixed 0.5 water-to-cement ratio (w/c) cement paste, made with CEM II/B-L32,5N [20] as illustrated in Figure 1. Afterward, the tip, now enclosed in a thin layer of cement paste with 150 µm of thickness, was placed in a sealed container, half filled with water. Thus, the cement paste was left to properly hydrate and cure in an atmosphere with an ample supply of water for seven days [21], which was achieved using pure water at room temperature.

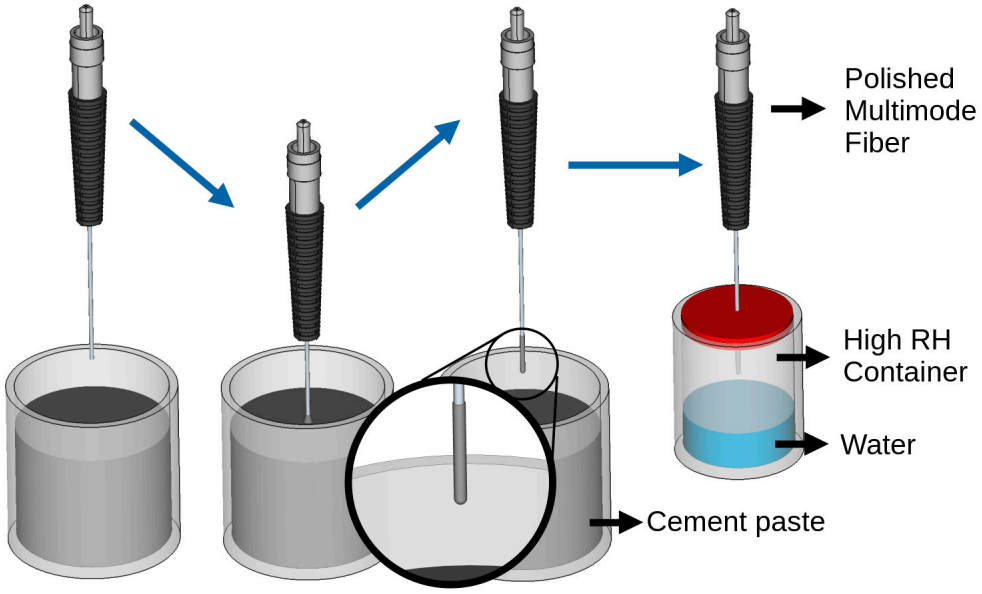

Figure 1. Cement paste sample production by dipping the fiber in cement paste and leaving it to cure in a closed container with water for a 7-day moist cure.

Hydrated cement paste, by virtue of its porosity, adsorbed and desorbed water according to the outside RH and its intrinsic properties. Light was guided through the optical fiber embedded in the cement paste (sensing fiber), and the reflected signal at the tip was heavily dependent on the quantity of water occupying the cement pores, Figure 2a. The refractive index (RI) of the pores changed between 1 and 1.33 depending on the amount of water that filled the pores [22]. A change in RI influenced light reflectance at the tip, with it being higher if the pores were dry and lower if the pores were filled with water.

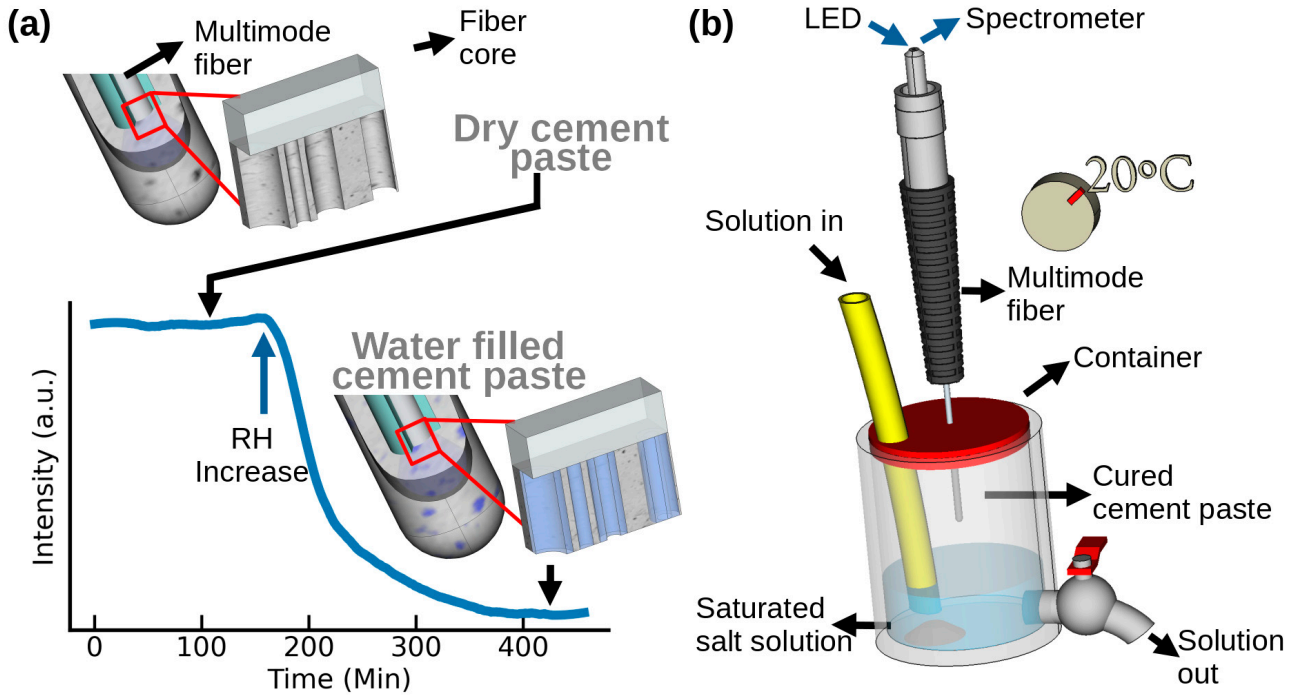

Figure 2. (**a**) Intensity loss due to the buildup of water in cement paste due to the increase in outside RH. (**b**) Experimental setup with a polished multimode fiber embedded in cement paste, placed in a closed container where saturated salt solutions are added and removed at 20 °C.

The light source used was a single light-emitting diode (LED-XSL-370-TB-5, Roithner LaserTechnik GmbH, Vienna, Austria) with peak emission at 375 nm, and the detector was a micro spectrometer (C12880MA, Hamamatsu, Shizuoka, Japan). These components were connected through a Y-shape fiber optic bundle, which comprised two multimode fibers with 200 µm core diameter (EOS-26488, Ocean Optics, Dunedin, FL, USA).

The sensing fiber was placed in a closed container into which a saturated salt solution was inserted, Figure 2b. At the end of the measurement, a valve at the bottom was opened for the removal of the saturated salt solution. Before the next saturated salt solution was introduced, the container was quickly rinsed with water three times to cleanse the previous solution and with care so as not to wet the cement paste. Salts used in this study covered RHs between 8.9 and 97.6% (20 °C), with water being used to achieve 100% RH, Table 1. The temperature was set at 20 °C throughout these measurements.

Table 1. Salts used for the saturated salt solutions and their respective RH [9].

Salt	%RH (20 °C)
Sodium Hydroxide	8.91
Sodium Bromide	59.14
Sodium Chloride	75.47
Potassium Chloride	85.11
Potassium Nitrate	94.62
Potassium Sulfate	97.59

Cement paste water sorption and desorption exhibited hysteretic behavior due to the cement paste's mesoporosity. Valuable information was gathered by studying both the adsorption and the desorption branches, but to do so, reflection light intensity needed to be related to an amount of water. Measured light intensity was comprised of two components, one that remained in the fiber and one that left the fiber. Light that left the fiber interacted with the cement paste, part of which was diffusely reflected towards the fiber tip and part of which was absorbed by the cement paste. Light that left the fiber remained stable throughout this monitoring due to the cement paste's stability and the very low spectral absorbance of water at 388–400 nm [23], Figure 3, wavelengths over which light intensity was integrated throughout this work.

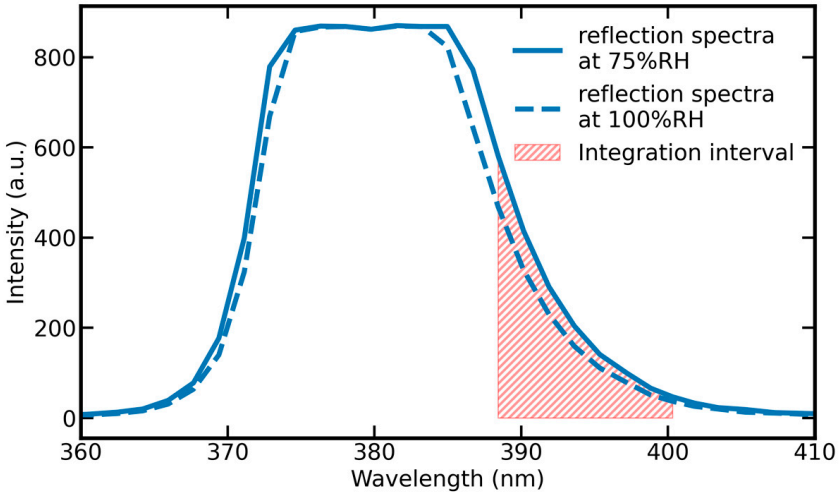

Figure 3. Raw reflected light spectra for RHs between 75% and 100% and the integration interval used between 388 and 400 nm.

Light that remained in the fiber by being reflected at the tip interface changed according to the area of water, a_w, that was filling the area of cement pores, a_p, in contact with the fiber tip. The area of the probe was that of the fiber tip, $a_c = \pi 0.3^2$ cm^2, whose core was

600 µm in diameter. Measured light intensity, $I_M(a_w)$, is a linear function of a_w, with $I_{max} = I_M(0)$ and $I_{min} = I_M(a_p)$, Equation (1).

$$I_M(a_w) = \frac{I_{min} - I_{max}}{a_p} a_w + I_{max} \quad (1)$$

A large component of the measured signal was light being diffusively reflected when it interacted with the cement paste, which were removed from the analysis by normalizing the signal, $I_N(a_w)$, Equation (2).

$$I_N(a_w) = -\frac{I_M(a_w) - I_{max}}{I_{max} - I_{min}} = \frac{a_w}{a_p} \quad (2)$$

$I_N(a_w)$ portrays the amount of water that fills the capillary pores, and this relationship is used in the estimation of the $\%water\ mass$, which is the ratio between the weight of water (w_w) and the weight of cement paste (w_c). The weight of cement paste remains static throughout these measurements and is defined by the cement paste's volume (v_c), porosity (ϕ), and relative density (ρ_c). The weight of water depends on how much water fills the cement pores, which is given by $I_N(a_w)$. The volume of cement pores depends on cement paste volume (v_c) and porosity (ϕ). The aforementioned relationships are displayed in Equation (3).

$$\%water\ mass = \frac{w_w}{w_c} = \frac{v_c * \phi * I_N}{(1-\phi) v_c \rho_c} = \frac{\phi}{(1-\phi)\rho_c} I_N \quad (3)$$

2.1. Brunauer-Emmett-Teller

The Brunauer-Emmett-Teller (BET) method [10] was used when surface adsorption occurs in multimolecular layers without capillary condensation; this is valid for relative humidities between 5% and 40%. In this region, it is possible to estimate the volume of water required to cover the absorbent's surface with a monomolecular layer of water (v_m), Equation (4), considering a high value of enthalpy of adsorption [8].

$$v_m = v_w(1-h) = I_N v_c \phi (1-h) \quad (4)$$

v_m is achieved by measuring the volume of water (v_w) for relative humidity (h) between 5% and 40%. The volume of water, as measured by light reflectance, is defined by $I_N v_c \phi$, which was previously used in Equation (3). There is no estimation for the volume of cement (v_c) that maintains a good relation to the area of cement paste in direct contact with the optical fiber core. For this reason, it was not possible to estimate v_m through reflected light intensity, as it would be if gravimetric or volumetric measurements were being performed. For the same reason, the measurements of total surface area (TSA) were beyond the reach of this setup. TSA is calculated by converting v_m into the number of molecules of water and multiplying it by the area covered by each one,

$$TSA = \frac{A_m v_m N_A}{V_M} \quad (5)$$

wherein V_m is the molar volume, N_A is Avogadro's number, and A_m is the area occupied by each molecule of absorbed water.

It is possible to estimate the specific surface area of cement paste, S_{BET}, which is calculated by dividing TSA by the weight of cement paste (w_c) as seen in Equation (6).

$$S_{BET} = \frac{TSA}{w_c} = \frac{A_m N_A}{V_M} I_{N8.9}(1-h) \frac{\phi}{\rho_c(1-\phi)} \quad (6)$$

In the current work, this value was estimated with normalized reflected light intensity at 8.9% RH, $I_{N8.9}$, achieved through a saturated salt solution of sodium hydroxide. Furthermore, I_N at any RH can be converted through TSA into the thickness of water, $t(h)$.

$$t(h) = \frac{v_w}{TSA} = \frac{I_N}{I_{N8.9}} \frac{V_M}{A_m N_A (1-h)} \tag{7}$$

$t(h)$ estimated through reflected light intensity can be compared with values found in the literature, validating the setup and methodology employed [10].

2.2. Barret-Joyner-Halenda

The Barret-Joyner-Halenda (BJH) method estimates the pore size distribution through the step-by-step analysis of water vapor desorption [24]. It assumes that two mechanisms of water vapor desorption are working concurrently: physical desorption from the pore walls and capillary evaporation. It also assumes the pores to be cylindrical in shape [8]. Physical desorption is linked to $t(h)$, which lowers with the decrease of RH [25]. Capillary evaporation depends on changes in vapor pressure at a curved liquid-vapor interface. This is displayed in the Kelvin-Laplace equation, Equation (8), which sets the radius of liquid menisci for a given RH, kelvin radius (r_k).

$$r_K(h) = -\frac{2\sigma V_M}{RTln(h)} \tag{8}$$

where σ is the surface tension of the liquid, R is the universal gas constant, and T is the temperature. Pores with a radius, r_p, smaller than $r_K(h) + t(h)$, remained filled with water. Pores with a $r_p > r_K(h) + t(h)$, contained only a layer of water that follows $t(h)$. r_p is calculated through Equation (9).

$$r_p = r_K(h) + t(h) \tag{9}$$

As the RH is successively reduced, the area of water (value measured through reflected light intensity) that is evaporated is related to pores with a given r_p. Hence, a change in the area of water, Δa_w, due to a reduction of RH is related to the area occupied by pores, Δa_p, whose r_p are between the previous and the current values of relative humidity, Δr_p. The process of estimating Δa_p, begins by converting I_N into a_w, Equation (10).

$$a_w = a_c \phi I_N \tag{10}$$

where Δa_w is influenced by two groups of pores. The first group has pores, whose menisci broke in the present reduction of relative humidity, which relates to Δa_p through R, defined in Equation (11).

$$R = \frac{r_p^2}{(r_K(h) + \Delta t(h))^2} \tag{11}$$

where $\Delta t(h)$ is the change in the thickness of water caused by the decrease in RH. The second group of pores that influence Δa_w is the pores whose menisci were already broken before the current reduction in RH. These pores will influence Δa_w through reductions in water thickness at the pore walls. The change in the area attributed to this, $\Delta a_{\Delta t}$, is equivalent to a ring with the current $\Delta t(h)$, Equation (12).

$$a_{\Delta t} = \pi(r_K + \sum_{i=1}^{n} \Delta t_i)2 - \pi(r_K + \sum_{i=1}^{n-1} \Delta t_i)2 \tag{12}$$

The sums of Equation (12) represent the total change in thickness due to the changes in RH that have taken place up until this point, with n being the current number of RH changes. The number of pores that exerts this influence increases with each reduction of

RH. For each Δr_p that has been computed, there is a $a_{\Delta t}$ that will influence the following measures of Δa_w; they are, for this reason, summed and removed in Equation (13), resulting in the Δa_p.

$$\Delta a_p = R\left(\Delta a_w - \sum_{i=1}^{n-1} a_{\Delta t}\right) \quad (13)$$

Pore size distribution is displayed in this work as $\Delta a_p/\Delta r$, given that I_N relates to the area of desorbed water, Δa_w. In the literature, which employs gravimetric or volumetric measurements, pore size distribution is displayed by $\Delta V/\Delta r$ since it is the volume of water being measured for each successive reduction of relative humidity.

3. Results and Discussion

The importance of the seven-day moist cure of the cement paste sample in an atmosphere with an ample supply of water is shown in Figure 4. The cement paste cured under a moist environment for seven days was cohesive, as seen in Figure 4a, unlike the sample left to cure in the air, which displayed large cracks, Figure 4d. The stability of the signal was also influenced by the cure of the sample. The seven-day moist cure cement paste sample maintained stable values of reflected light intensity for ambient and 100% RH, Figure 4b,c, unlike the air-cured sample, Figure 4e,f. These intensities were achieved by integrating reflected light intensity over the wavelengths of 388–400 nm, the same interval seen in Figure 3.

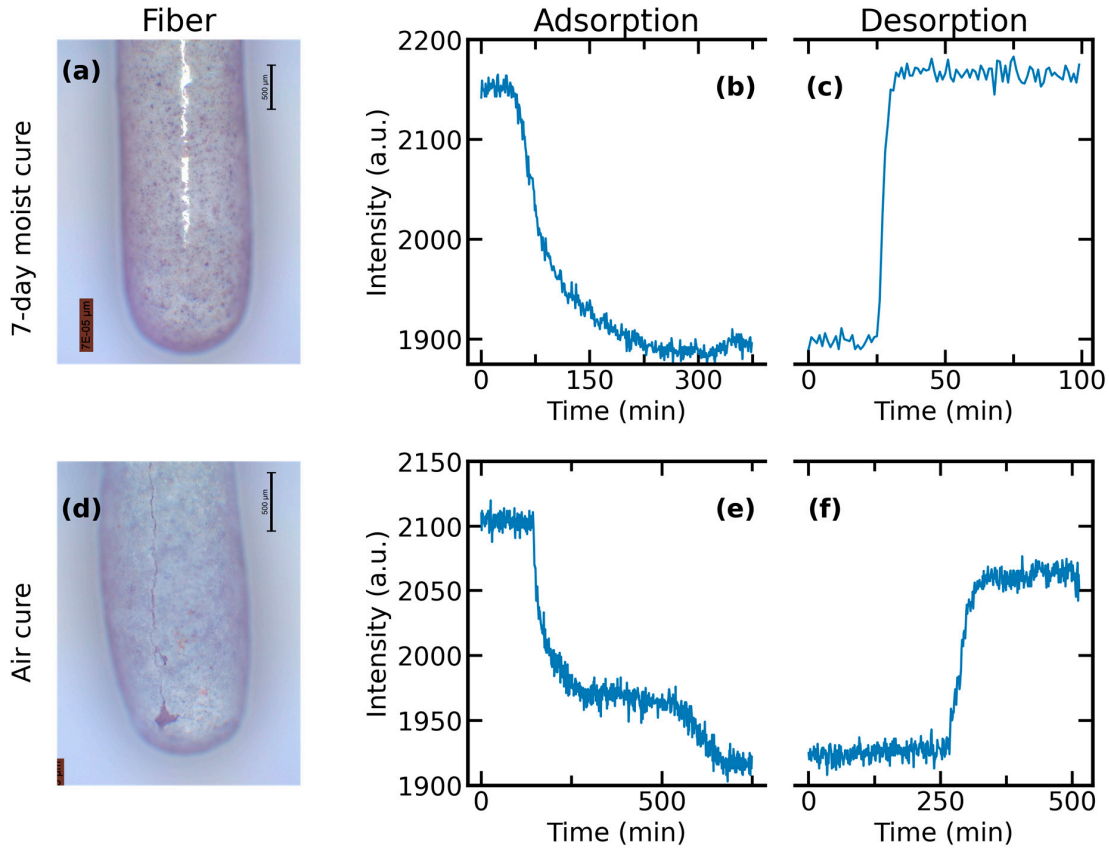

Figure 4. (**a**) Image of the seven-day moist cured cement paste around the multimode optical fiber. (**b**,**c**) are the adsorption and desorption between 100% RH and ambient RH for the seven-day moist cured cement paste. (**d**) Image of a cement paste sample left to cure in air, displaying large cracks. (**e**,**f**) are the adsorption and desorption branches between 100% RH and ambient RH for the air-cured cement paste.

Using 100% RH in the study of water vapor sorption was discarded for this setup, as it produces in these smaller samples the equivalent effect of submerging a larger sample of cement paste in water: a rise in the *%water mass* of the desorption branch [12]. This can be seen in Figure 5, where the value of 100% RH is far above the others in intensity. At this RH, the cement paste sample is covered by a water droplet, which is roughly the same thickness as the cement paste sample. For this reason, the maximum value of RH employed was 97.6%. Figure A1 contains the raw data, as well as the data points selected for the analysis of Figure 5a.

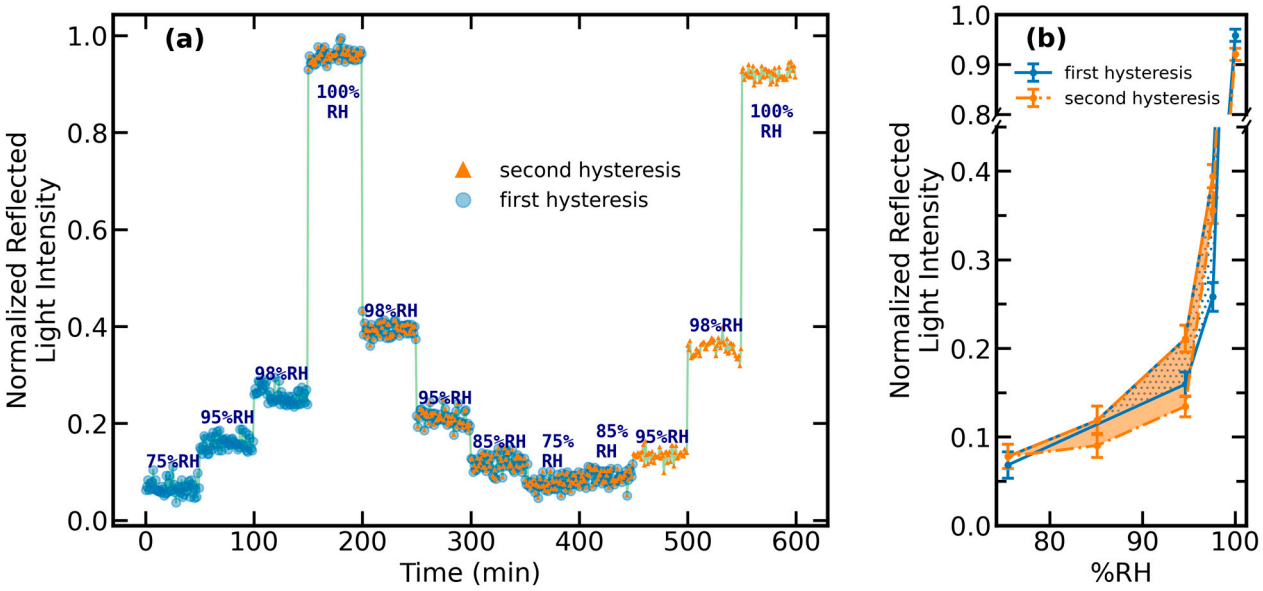

Figure 5. (**a**) Normalized reflected light intensities for different RH between 75% and 100%. The values of 75%, 85%, 95%, and 98% are rounded values from Table 1. (**b**) The two-resulting hysteresis.

Water vapor sorption characterization began by converting the reflected light intensity into *%water mass* through Equation (3), Figure 6a,b. The porosity of 0.5 w/c in bulk cement paste is 22% [4], but cement paste's porosity increases the closer it is to an aggregate [26], which, in this case, was the optical fiber. Hence the chosen value of ϕ to be used in Equation (3) was 37%. Figure A2 contains the raw data, as well as the data points selected for the analysis in Figure 6a.

By analyzing the desorption branch through the BET method, Equation (6), the specific surface area of the cement paste sample was found to be 133 m^2/g, which is close to the ones found in the literature (123 m^2/g for 0.45 w/c [10]). Normalized light intensity was converted through Equation (7) into the thickness of water and compared to the literature [25], Figure 6c. The calculated values of water thickness fall close to the expected ones, but the curve deviated from the expected. Measurements of water thickness through cement paste samples were expected to go above those found in the literature for $RH > 63\%$, where adsorption was now dominated by capillary condensation to the detriment of multilayer adsorption [7]. Fiber tip data only goes above the thickness of water due to multilayer adsorption for $RH > 95\%$, which indicates larger pores are delaying capillary condensation since they require larger values of RH for it to occur. Decreasing the increments of RH, among other improvements to the measuring setup and decreasing the w/c of the cement paste, might improve this response.

From the BJH method, the expected trend was found in the pore size distribution: an increase in $\Delta a_p/\Delta r$ for decreasing pore radius, Figure 6d. A more pronounced increase between the intervals of [2.6, 4.6 nm] and [0.6, 2.6 nm] was found in [10] than in the fiber tip data. This was expected given the thin nature of this cement paste sample and the presence of the optical fiber in the middle, which works as an aggregate, further increasing the porosity of the sample [26]. The large decrements in RH did not allow for a better

analysis of the pore distribution between 4.6 and 20.6 nm pore radius. It, however, seems to be in line with those reported in the literature for this pore radius [10,27].

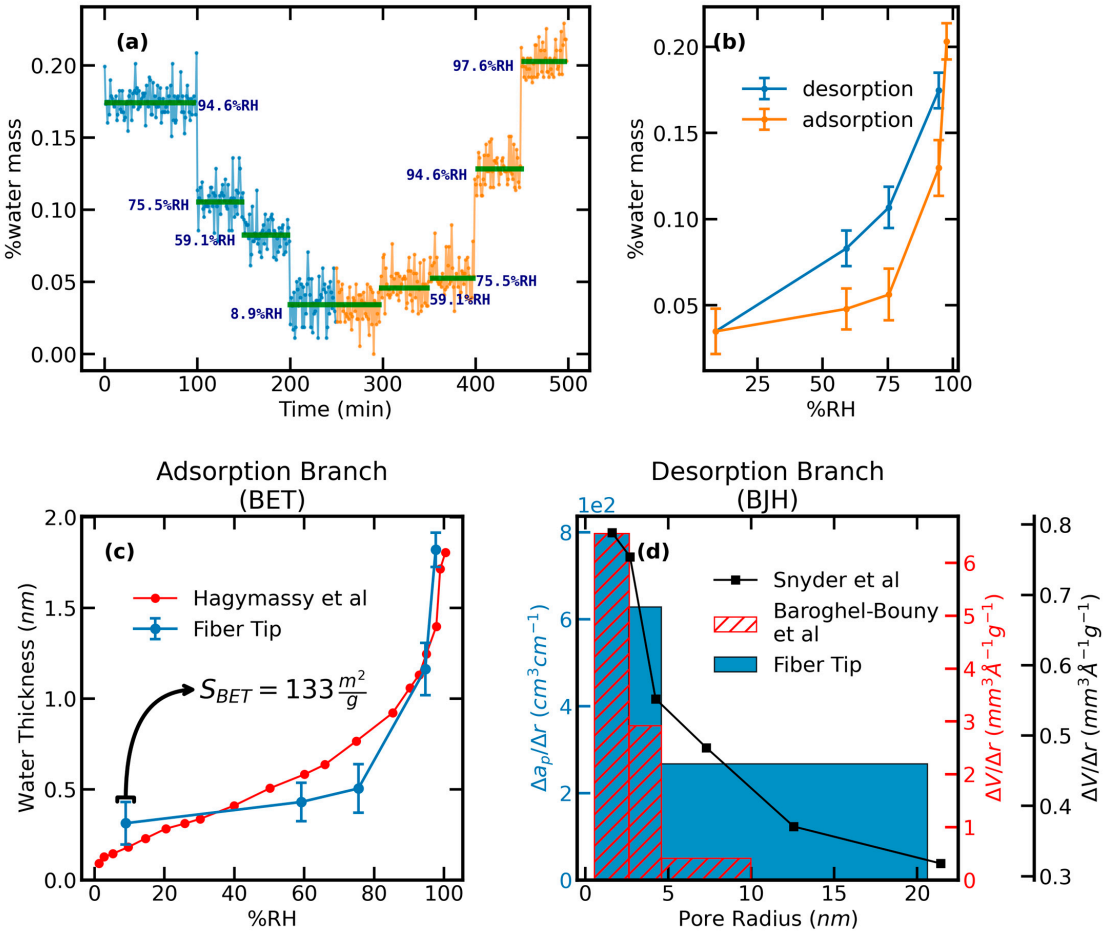

Figure 6. (**a**) *%water mass* from the normalized reflected light intensity for each of the saturated salt solutions used and the hysteretic behavior of the cement paste (**b**). (**c**) Estimated specific surface area and thickness of water retrieved from the adsorption branch of the cement paste water vapor hysteresis. Computed thickness of water (nm**)** is compared to the values found in the literature [25]. (**d**) Pore size distribution calculated from the desorption branch of the normalized reflected light intensity compared to values found in the literature [10,27].

As it stands, sorption isotherms through light reflectance can achieve two main objectives: specific surface area and pore size distribution. Unfortunately, this method cannot compute the porosity of the sample, nor can it achieve the values of v_m and TSA, which are achievable through volumetric and gravimetric methods of sorption isotherms. In terms of sample preparation, light reflectance is akin to gravimetric measurements; it does not require pretreatment, unlike volumetric measurements. As of this work, light reflectance can only be used with new cement paste samples, which are cured with an embedded multimode fiber, whilst gravimetric and volumetric methods can be used in samples retrieved from existing infrastructure. In terms of data acquisition time, light reflectance is as fast or faster than dynamic vapor sorption while having a simpler system of maintaining a stable value of RH based on saturated salt solutions. Similar to dynamic vapor sorption, this method allows for real-time monitoring of water sorption hysteresis. In terms of data interpretation, the fast data acquisition time should be taken into consideration, given the differences that arise between long-term/short-term water vapor sorption [13]. It is also worth considering that light reflectance only monitors the entrance of the pores; hence, it

could be monitoring the size of pore entry as in MIP measurements [28], with the latter having the disadvantage of being a destructive method [13].

4. Conclusions

A multimode fiber was used to monitor the water vapor sorption hysteresis of a small cement paste sample through changes in reflected light intensity, which happened due to changes in the quantity of water in the cement paste pores. The proper curing of the cement paste sample is key in achieving stable values of reflected light intensity and good adsorption and desorption behaviors. At 100% RH, the cement paste sample is submerged by a water droplet, which increases the amount of normalized reflected light intensity beyond what is expected from water vapor adsorption. This study of water vapor sorption hysteresis was conducted for RHs between 8.9 and 97.6%, considering a porosity of 37%. Using the BET method, the specific surface area of cement paste was calculated to be 133 m^2/g, and the thickness of water for each value of relative humidity was close to the ones found in the literature. Through the BJH method, pore size distribution was achieved for pore radii between 0.6 and 20.6 nm, with an increase in prevalence towards smaller pores; the highest value of $\Delta a_p/\Delta r$ was achieved in the 0.6–2.6 nm interval, behavior which was also found in the literature.

Author Contributions: Conceptualization, P.M.d.S., L.C.C.C. and J.M.M.M.d.A.; Methodology, P.M.d.S.; Software, P.M.d.S.; Formal Analysis, P.M.d.S.; Resources, P.M.d.S. and L.C.C.C.; Data Curation, P.M.d.S.; Writing—Original, P.M.d.S.; Visualization, P.M.d.S.; Funding Acquisition, L.C.C.C., J.M.M.M.d.A.; Writing—Review & Editing, L.C.C.C., J.M.M.M.d.A. All authors have read and agreed to the published version of the manuscript.

Funding: This work is financed by National Funds through the Portuguese funding agency, FCT—Fundação para a Ciência e a Tecnologia, within the Ph.D. grant UI/BD/152695/2022 and the research contract CEECIND/00471/2017.

Institutional Review Board Statement: Not applicable.

Informed Consent Statement: Not applicable.

Data Availability Statement: The data used in this work is available upon request.

Conflicts of Interest: The authors declare no conflict of interest.

Appendix A

Raw data from the reflected light intensity used to analyze the effect of placing the cement paste samples under 100% RH, as seen in Figure 5, is presented in Figure A1.

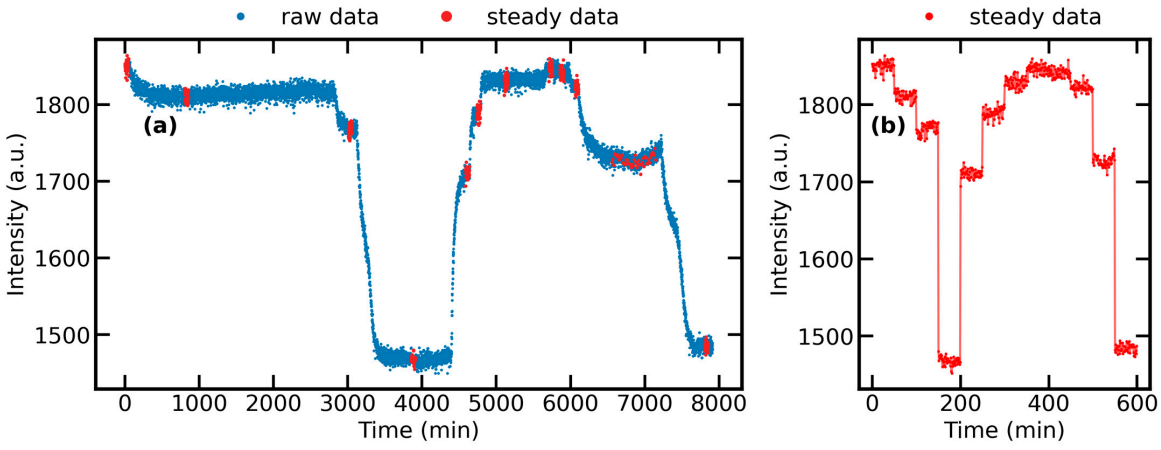

Figure A1. (**a**) Raw reflected light intensities for different RH between 75% and 100%, achieved by integrating between the wavelengths of 388 and 400 nm (**b**) chosen stable points for analysis.

Raw data from the reflected light intensity used for the characterization of cement paste through sorption isotherm, as seen in Figure 6, is presented in Figure A2.

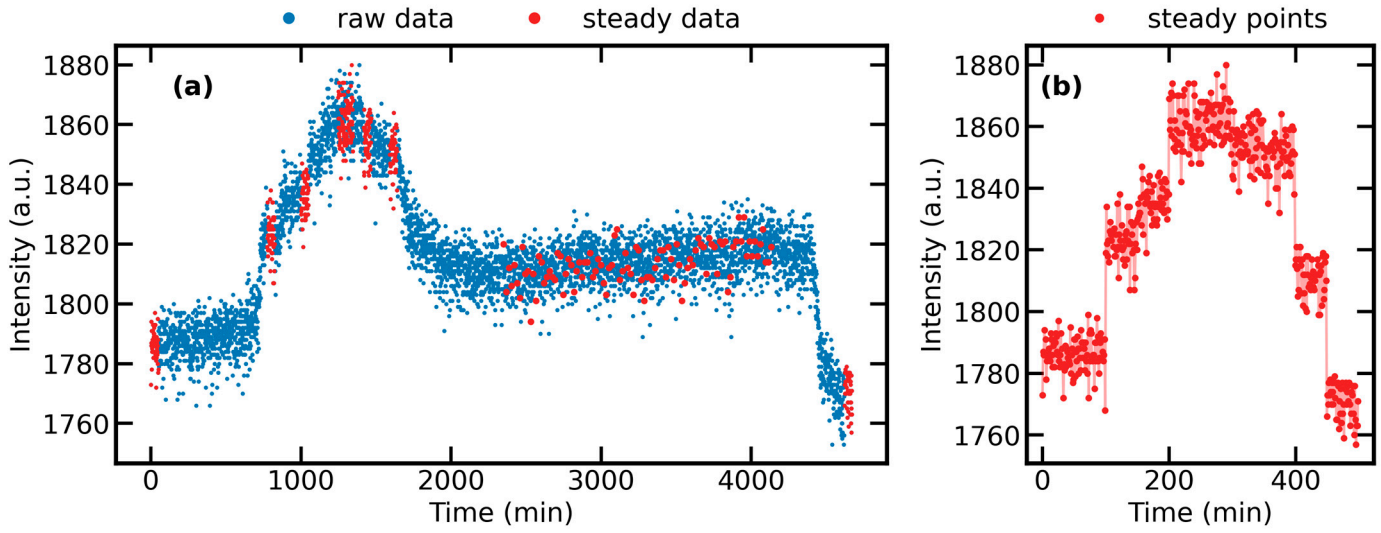

Figure A2. (**a**) Raw reflected light intensities for different RH between 8.9 and 97.6% and (**b**) the chosen stable points for analysis. Results were achieved by integrating intensities between 388 and 400 nm.

References

1. *UNECE Carbon Neutral Energy Intensive Industries*; Information Service United Nations Economic Comission for Europe: Geneva Switzerland, 2022.
2. Aıtcin, P.-C. Cements of Yesterday and Today. *Cem. Concr. Res.* **2000**, *30*, 1349–1359. [CrossRef]
3. Lynch, J.P.; Farrar, C.R.; Michaels, J.E. Structural Health Monitoring: Technological Advances to Practical Implementations [Scanning the Issue]. *Proc. IEEE* **2016**, *104*, 1508–1512. [CrossRef]
4. Mehta, P.K.; Monteiro, P.J.M. *Concrete: Microstructure, Properties, and Materials*; McGraw Hall India: Uttar Pradesh, India, 2005; ISBN 0071462899.
5. Taylor, P.C. *Curing Concrete*; CRC Press: Boca Raton, FL, USA, 2013; ISBN 9780203866139.
6. Baroghel-Bouny, V. Water Vapour Sorption Experiments on Hardened Cementitious Materials. Part II: Essential Tool for Assessment of Transport Properties and for Durability Prediction. *Cem. Concr. Res.* **2007**, *37*, 438–454. [CrossRef]
7. Baroghel-Bouny, V. Water Vapour Sorption Experiments on Hardened Cementitious Materials. *Cem. Concr. Res.* **2007**, *37*, 414–437. [CrossRef]
8. Sing, K.S.W. Reporting Physisorption Data for Gas/Solid Systems with Special Reference to the Determination of Surface Area and Porosity (Recommendations 1984). *Pure Appl. Chem.* **1985**, *57*, 603–619. [CrossRef]
9. Greenspan, L. Humidity Fixed Points of Binary Saturated Aqueous Solutions. *J. Res. Natl. Bur. Stand. A Phys. Chem.* **1977**, *81A*, 89. [CrossRef]
10. Baroghel-Bouny, V.; Chaussadent, T. Texture and Moisture Characterization of Hardened Cement Pastes and Concretes from Water Vapour Sorption Measurements. In *The Modelling of Microstructure and Its Potential for Studying Transport Properties and Durability*; Jennings, H., Kropp, J., Scrivener, K., Eds.; Springer: Dordrecht, The Netherlands, 1996; pp. 241–255. ISBN 978-90-481-4653-6.
11. Muller, A.C.A. Characterization of Porosity & C-S-H in Cement Pastes by 1 H NMR. Ph.D. Thesis, École Polytechnique Fédérale De Lausanne, Lausanne, Switzerland, 2014.
12. Wu, M.; Johannesson, B.; Geiker, M. A Study of the Water Vapor Sorption Isotherms of Hardened Cement Pastes: Possible Pore Structure Changes at Low Relative Humidity and the Impact of Temperature on Isotherms. *Cem. Concr. Res.* **2014**, *56*, 97–105. [CrossRef]
13. Aili, A.; Maruyama, I. Review of Several Experimental Methods for Characterization of Micro- and Nano-Scale Pores in Cement-Based Material. *Int. J. Concr. Struct. Mater.* **2020**, *14*, 55. [CrossRef]
14. Jennings, H.M. A Model for the Microstructure of Calcium Silicate Hydrate in Cement Paste. *Cem. Concr. Res.* **2000**, *30*, 101–116. [CrossRef]
15. Chen, X.; Triquet, J.; Sanchez, T.; Pathirage, M.; Conciatori, D.; Sorelli, L.; Cusatis, G. *An Experimental Study on the Sorption in UHPFRC: Adaptation of the DVS Measurement Procedure*; Springer International Publishing: Cham, Switzerland, 2022; pp. 1278–1285.
16. Maaroufi, M.; Belarbi, R.; Abahri, K.; Benmahiddine, F. Full Characterization of Hygrothermal, Mechanical and Morphological Properties of a Recycled Expanded Polystyrene-Based Mortar. *Constr. Build. Mater.* **2021**, *301*, 124310. [CrossRef]

17. Nguyen, H.T.; Rahimi-Aghdam, S.; Bažant, Z.P. Sorption Isotherm Restricted by Multilayer Hindered Adsorption and Its Relation to Nanopore Size Distribution. *J. Mech. Phys. Solids* **2019**, *127*, 111–124. [CrossRef]
18. Jiang, Z.-L.; Pan, Y.-J.; Lu, J.-F.; Wang, Y.-C. Pore Structure Characterization of Cement Paste by Different Experimental Methods and Its Influence on Permeability Evaluation. *Cem. Concr. Res.* **2022**, *159*, 106892. [CrossRef]
19. Gartner, E.; Maruyama, I.; Chen, J. A New Model for the C-S-H Phase Formed during the Hydration of Portland Cements. *Cem. Concr. Res.* **2017**, *97*, 95–106. [CrossRef]
20. MAESTRO CEM II/B-L 32.5N. Available online: https://www.secil.pt/en/products/cement-and-lime/grey-cement/maestro-cem-ii-b-l-32-5n (accessed on 28 December 2022).
21. ACI (American Concrete Institute). *Guide to External Curing of Concrete*; ACI 308R-16; American Concrete Institute: Farmington Hills, MI, USA, 2016; Available online: https://www.concrete.org/portals/0/files/pdf/previews/308r_16_preview.pdf (accessed on 28 December 2022).
22. da Silva, P.M.; Coelho, L.C.C.; de Almeida, J.M.M.M. Single Fiber Reflectance Spectroscopy for the Monitoring of Cement Paste. *Chemosensors* **2021**, *9*, 312. [CrossRef]
23. Hale, G.M.; Querry, M.R. Optical Constants of Water in the 200-Nm to 200-Mm Wavelength Region. *Appl. Opt.* **1973**, *12*, 555. [CrossRef] [PubMed]
24. Barrett, E.P.; Joyner, L.G.; Halenda, P.P. The Determination of Pore Volume and Area Distributions in Porous Substances. I. Computations from Nitrogen Isotherms. *J. Am. Chem. Soc.* **1951**, *73*, 373–380. [CrossRef]
25. Hagymassy, J.; Brunauer, S.; Mikhail, R.S. Pore Structure Analysis by Water Vapor Adsorption. *J. Colloid Interface Sci.* **1969**, *29*, 485–491. [CrossRef]
26. Scrivener, K.L.; Crumbie, A.K.; Laugesen, P. The Interfacial Transition Zone (ITZ) Between Cement Paste and Aggregate in Concrete. *Interface Sci.* **2004**, *12*, 411–421. [CrossRef]
27. Snyder, K.A.; Winslow, D.N.; Bentz, D.P.; Garboczi, E.J. Effects of Interfacial Zone Percolation on Cement-Based Composite Transport Properties. *MRS Proc.* **1991**, *245*, 265. [CrossRef]
28. Mercury Intrusion Porosimetry. In *A Practical Guide to Microstructural Analysis of Cementitious Materials*; CRC Press: Boca Raton, FL, USA, 2018; pp. 438–463.

Disclaimer/Publisher's Note: The statements, opinions and data contained in all publications are solely those of the individual author(s) and contributor(s) and not of MDPI and/or the editor(s). MDPI and/or the editor(s) disclaim responsibility for any injury to people or property resulting from any ideas, methods, instructions or products referred to in the content.